Chirality Screening and Metastable States in Chiral Nematic Colloids

V. S. R. Jampani,[1] M. Škarabot,[1,2] S. Čopar,[2] S. Žumer,[1,2] and I. Muševič[1,2]
[1]Jožef Stefan Institute, Jamova 39, 1000 Ljubljana, Slovenia
[2]Faculty of Mathematics and Physics, University of Ljubljana, Jadranska 19, 1000 Ljubljana, Slovenia
(Received 24 September 2012; published 23 April 2013)

We show that forces between two colloidal particles in a thin layer of a chiral nematic liquid crystal strongly depend on the chirality of the liquid crystal. The observed pair potentials are attractive, but are oscillatory functions of colloidal separation. The number and the position of local energy minima increase with increasing chirality. The pair interaction is the strongest for the pitch equal to the colloidal diameter and decreases with increasing chirality. We show that the chirality of the medium is responsible for this oscillatory nature and screening of the colloidal interaction in the far and near field. The measurements are in agreement with numerical calculations using Landau–de Gennes theory.

DOI: 10.1103/PhysRevLett.110.177801 PACS numbers: 61.30.−v, 61.30.Jf, 64.70.pv

Topology and interactions [1] of colloidal particles in liquid crystals [2] (LCs) have attracted significant interest in recent years because of the rich variety of unusual fundamental phenomena observed in these systems. It was demonstrated in a number of experiments that the chirality has a profound impact on the nature of nematic colloidal interactions. Chirality is responsible for vortex-like topological defects that mediate chiral nematic colloidal interaction [3]. These are nonsingular defects with -2 topological charge that are similar to the magnetic hyperbolic vortices [4]. Recently discovered torons [5] are toruslike, -2 topological charge objects that are optically induced in a frustrated chiral nematic LC. Knots and links of closed topological defect loops can exist only in chiral nematic LC colloids, as demonstrated recently [6,7]. Numerical studies of chiral nematic colloids [8,9] predicted self-assembly and nonlinear dynamics of dimeric colloidal rotors [10]. Chirality is also responsible for interesting material properties of chiral nematic dispersions, such as reconfigurable colloidal interaction in chiral nematics in 3D [11], solidlike elasticity in long-pitch cholesterics [12,13] and particle segregation and layering in short-pitch cholesterics [14].

In this Letter we show that chirality of the force-mediating medium is responsible for the oscillatory nature and screening of pair-interaction force in 2D chiral nematic colloids. We demonstrate the existence of local energy minima in the colloidal pair-interaction landscape and screening of the interaction in both the near field and far field. These are new phenomena that are not observable in nonchiral nematic colloids and are attributed solely to the chirality of the system.

We used silica particles with a diameter of $d = 4.7$ μm (Bangs Laboratories, Inc.), treated with DMOAP (octadecyldimethyl (3-trimethoxysilylpropyl) ammonium chloride, ABCR), to obtain strong perpendicular surface anchoring of LC molecules [15]. The colloids were dispersed in 5CB (Nematel), doped with right-handed CB15 (Merck), to induce chiral nematic phase of variable pitch p. Glass cells were assembled from two indium-tin-oxide (ITO) coated 0.7 mm thick glass slides, covered with a thin layer of a polyimide (PI-2555, NISSAN Chemicals). The polyimide layer was rubbed unidirectionally to obtain planar alignment of doped 5CB, with alignment on both surfaces set parallel. CB15 concentration was adjusted to the LC layer thickness h to obtain nematic structures, twisted by multiples of half-pitch, $h = N(p/2)$ in glass cells (denoted as $N\pi$ cells) with a gap of $h \sim 5$–6 μm, controlled with mylar spacers. Chiral nematic dispersion was introduced into the glass cell by capillarity at room temperature. Colloidal particles did not stick to the surface because of elastic repulsion between surfaces inducing planar anchoring and particles enforcing homeotropic alignment. To observe and manipulate the colloidal particles in the LC, we used 1064 nm laser tweezers (Aresis, Tweez 70) built around an inverted microscope (Nikon Eclipse, TE2000-U). The trajectories of the particles were video recorded with Pixelink PLA 741 camera at 40 fps. The positions of the particles were determined by a video-tracking procedure with a resolution of particle's position of ± 10 nm [16]. Having the time evolution of the trajectories, the force driving particle movement was determined as described in Ref. [17].

The forces between colloidal particles were measured by positioning a selected pair at a starting center-to-center separation of several μm. After switching off the traps, the movement of the particles was video monitored. In addition to highly anisotropic trajectories of particles, also observed in non-chiral nematic [18,19], we observe in chiral nematic LC a new phenomenon, illustrated in Fig. 1. Snapshots of the colloidal pair in the 2π cell in Fig. 1(a) indicate that during the time interval 120–360 s, the separation between the two particles does not change substantially. Brownian motion of particles is observed, but they are just wandering in close separation as if they experienced a local energy minimum. The same is

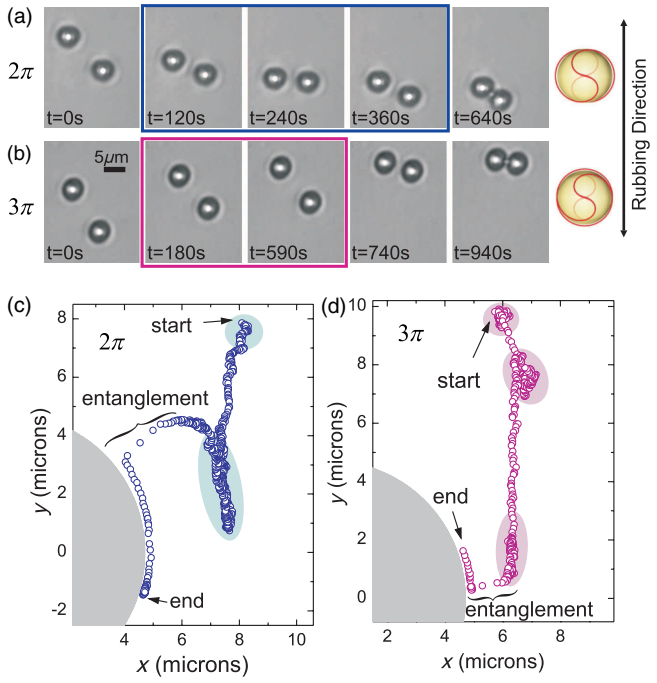

FIG. 1 (color online). Colloidal pair attraction in chiral nematic cells. (a) Snapshots of a colloidal pair in a 2π-cell demonstrate metastable states in the pair interaction. Between ~120 and ~360 s the particles fluctuate at a practically fixed separation. (b) In 3π cell the two particles are temporarily bound between ~180 and ~600 s. (c) Trajectory of a particle approaching the second particle in 2π cell. The particles' separation is measured from center to center. Shaded regions indicate metastable states. (d) Colloidal trajectory in a 3π cell reveals three metastable regions.

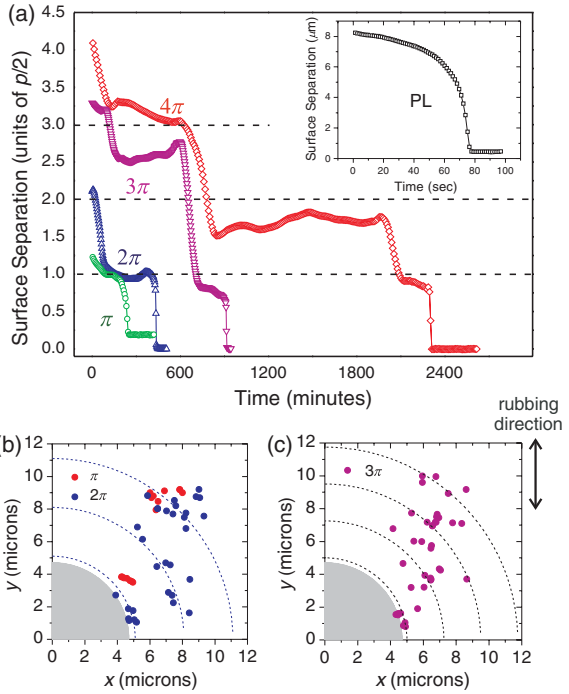

FIG. 2 (color online). Metastable and stable states in the pair interaction potential for chiral nematic colloids. (a) The time evolution of the surface-to-surface separation of a pair of colloidal particles with diameter 4.7 μm in a chiral NLC with variable chirality. The inset shows a colloidal attraction for a planar, homogeneous nematic LC. (b), (c) Distribution of observed colloidal metastable states in the plane, parallel to the layer of the chiral NLC. Each point denotes an observed (meta) stable state from different experiments.

observed for higher chirality, i.e., 3π cells, illustrated in Fig. 1(b).

The existence of local minima in the particles' pair interaction in chiral nematic cells is clearly revealed from their trajectories. Figure 1(c) shows a trajectory of a 4.7 μm colloidal particle when approaching another identical particle in the 2π cell, positioned at the origin of the reference frame. The total time of the experiment was 500 sec, and the trajectory has a complex shape composed of weakly curved segments and areas shaded in Figs. 1(c) and 1(d), with sharp turns and even loops. A close inspection of the shaded areas reveals, that this is a region of a local energy minimum in the pair interaction. The two particles experience Brownian motion with slight fluctuation in their separation, as if they were temporarily caught in a shallow potential pot. After spending some time in this potential pot (typically 300 sec for 2π cells) thermal fluctuations would kick the particle out of the pot and it would then continue its approach to the second particle. Finally, the particles are strongly attracted at small (i.e., 2.5 μm) surface-to-surface separation, which is accompanied by spontaneous entanglement of the two particles. The entanglement is clearly observable as the two defect rings of the particles merge and rewire into a single defect loop, entangling and strongly binding the particles.

Whereas in π-chiral nematic structures a single metastable state of a colloidal pair was observed, a second local energy minimum is observed in 2π cells, as shown in Fig. 1(c). Additional local minima are observed for higher chirality, which is evident from the particles' trajectories, shown in Fig. 2(a). In all cases, the starting surface-to-surface separation was ~8 μm. Two facts are evident from the Fig. 2(a). First, the "strength" of the pair interaction decreases with increasing chirality, as the time needed for the two colloids to come into the final state is longer for higher chirality. This time is 80 sec in planar cells, 4 min in π cells, and 45 min in 4π cells. Second, the number of metastable states increases with increased chirality and the local energy minima are related to the pitch of the chiral nematic structure, as seen from Fig. 2(a).

As the experiments are very sensitive and susceptible to external stimuli (temperature change, LC flow), several experiments have been performed on different cells and different colloidal pairs. The analysis shows a nearly linearly increasing number of metastable states with increased chirality of the NLC. It seems that by increasing the chirality in terms of an extra half-pitch (therefore

adding an extra π twist), the system gains one additional metastable state. Figures 2(b) and 2(c) show the distribution of local minima, determined from a large number of experiments in π, 2π, and 3π structures. The minima are all grouped at $\sim 45°$ with respect to the rubbing direction and in panel (b) one can see they are indeed grouped at discrete steps from the central particle.

The energies of these metastable states in chiral NLCs were analyzed by calculating the work, done by the attractive colloidal force, mediated by the chiral nematic liquid crystal [20]. While in planar nematic LCs this is an easy task, because the liquid-crystal-mediated forces are much stronger than the random thermal forces, the Brownian motion makes more difficult the evaluation of the work in chiral nematic LC, where the forces are weak. We have overcome this problem by carefully smoothing the particle's trajectories and dropping out from the evaluation procedure the regions of local energy minima. We have analyzed the resulting error in the calculated pair potentials, which is of the order of $\sim$10–20%. The results are presented in Fig. 3(a), where the pair interaction potential is shown as a function of time. The metastable states are clearly observable as nearly flat parts of the energy-vs-time curve. Analysis of colloidal Brownian motion [21] in these metastable states shows that they are highly anisotropic and their depths are several $\sim k_B T$.

Overall, the experiments indicate that the colloidal interaction is the strongest when the helical period p is equal to the diameter of the colloid, $p \sim 2R$, and increased chirality results in a weaker colloidal pair interaction. A small portion of this decrease could be attributed to the decrease of the elastic constants by increased doping with chiral CB15, which decreases the nematic-isotropic transition temperature.

A more detailed analysis shows that the colloidal interaction can be separated into the far-field and near-field interaction. The range of near-field and far-field interaction strongly decreases with increasing chirality. To analyze the nature of the far-field part of the interaction, we determined for each chirality the critical starting separation, from which the two colloids are attracted. If the starting separation is larger than the critical, the colloids do not attract within a reasonable time of measurement (1 h in π to 5π cells, more than 7 h for 9π cells). From these measurements we have determined the critical separation-chirality diagram shown in Fig. 3(b), which clearly demonstrates that by increasing the chirality, the colloidal pair potential is "screened." We have excluded all other effects. The screening of the far-field interaction by increasing chirality can be explained by considering spatial dependence of the interaction, carrying the perturbation. At $N\pi$ turns of the director, the perturbation is a N-times scaled-down version of the field at π turns. This scaling of all the distances with the pitch, already observed in the positions of the metastable states (Fig. 2), makes the range of the interaction

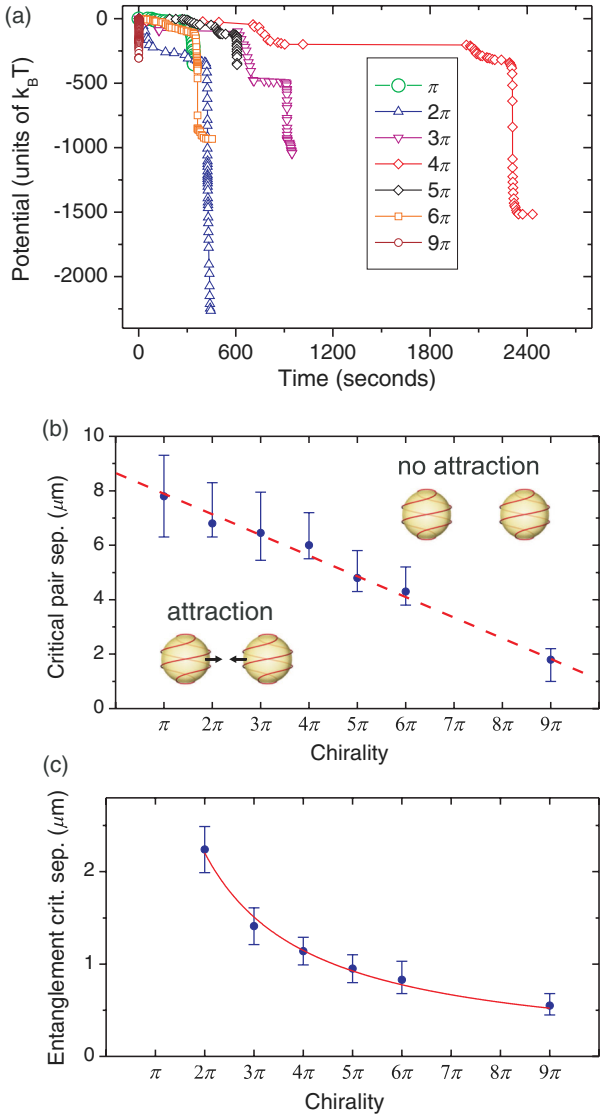

FIG. 3 (color online). (a) Potential energy of a 4.7 μm colloidal particle as a function of time, as it approaches to the second colloidal particle, shown for cells with different chirality. The potentials were calculated using data from Fig. 2. (b) Critical starting separation for a colloidal pair as a function of chirality. Dashed line is a guide to the eyes. (c) Critical separation of particles, where the entanglement starts to occur as a function of chirality. Solid line is a fit to the inverse helical pitch. In (b) and (c) chirality is measured in the total twist of the director field between the two confining surfaces.

shorter with increasing chirality. Similar screening of the pair interaction by chirality is observed in the near field. Figure 3(c) shows the critical separation, where the process of spontaneous entanglement starts, as the colloids are close enough. It should be stressed that in a nonchiral or weakly chiral nematic dispersions particle interaction is screened on scales determined by confinement.

The near-field colloidal pair interaction has been also analyzed for π cells using the Landau–de Gennes (LdG)

modeling with a finite difference relaxation method [22]. Because of the long range of the interaction and rather low intensity of the observed phenomena, a large simulation cell of $750 \times 750 \times 125$ has been used to avoid the unwanted interaction with the boundary. The potential profile has been calculated by repeating the simulation at different particle separations. Because of the computational complexity, a smaller system of a 900 nm particle in a 1150 nm cell was used, so only a qualitative agreement is expected.

The experimental results are shown in Fig. 4(a), and the corresponding calculated energy landscape is shown in Fig. 4(b) for the colloidal pair in the π cell. To test the anisotropy and search for the metastable states, the colloidal particle(s) was sequentially released from different starting positions, as numbered in Fig. 4(a). Starting positions 1, 2, 7, 10 are at the energy maxima, as the particle is repelled from its neighbor and driven to the metastable regions (encircled areas). On the contrary, particles released from the positions 3–5, 6, 8, 9 are attracted to the second particle. The numerical energy landscape is in qualitative agreement with experiments. It has two energy maxima along the rubbing direction, which are followed by two very deep energy minima at very small colloidal separation. Four energy minima are observed at $\sim 45°$, which match the local minima observed in π cells. It should be noted that the interaction between particles in chiral nematic liquid crystal has already been discussed theoretically by Fukuda *et al.* [23] in the limit when the particles are much smaller than the pitch. That work indicated that highly complex spatial pattern of the pairwise interaction energy in chiral media should be expected.

The emergence of shallow and localized energy minima in colloidal pair interaction can be qualitatively explained by considering the effect of the spherical particle on the helical arrangement of LC molecules. The homeotropic anchoring enforces local molecular orientation on the particles' surface that creates regions around each particle, where the uniform helical arrangement of molecules is slightly distorted. This is shown in Fig. 4(c), which presents the vertical position where the director twists by $\pi/2$ relative to the bottom of the cell. In a uniform helix, this happens at the middle of the cell, and deviation from this value signifies compression of the helix on one side and dilation on the other. The distortion of the helix is nonmonotonic with distance from the particle, and shows a single oscillation in the π cell. Because each particle is surrounded by a modulated region, local and very shallow energy minima occur if the directions of the distortions of both particles match [Fig. 4(d)]. For other directions of approach there is no such matching of the distorted regions and the particles repel, as can be seen from the energy pair potential landscape in Fig. 4(b).

In conclusion, spatial modulation and screening of the intercolloidal interaction, as reported in this work, are the two phenomena, whose origin can be traced back to the chirality of the liquid crystal medium. This is another example from a long series of chiral nematic colloidal phenomena, which demonstrates the importance of

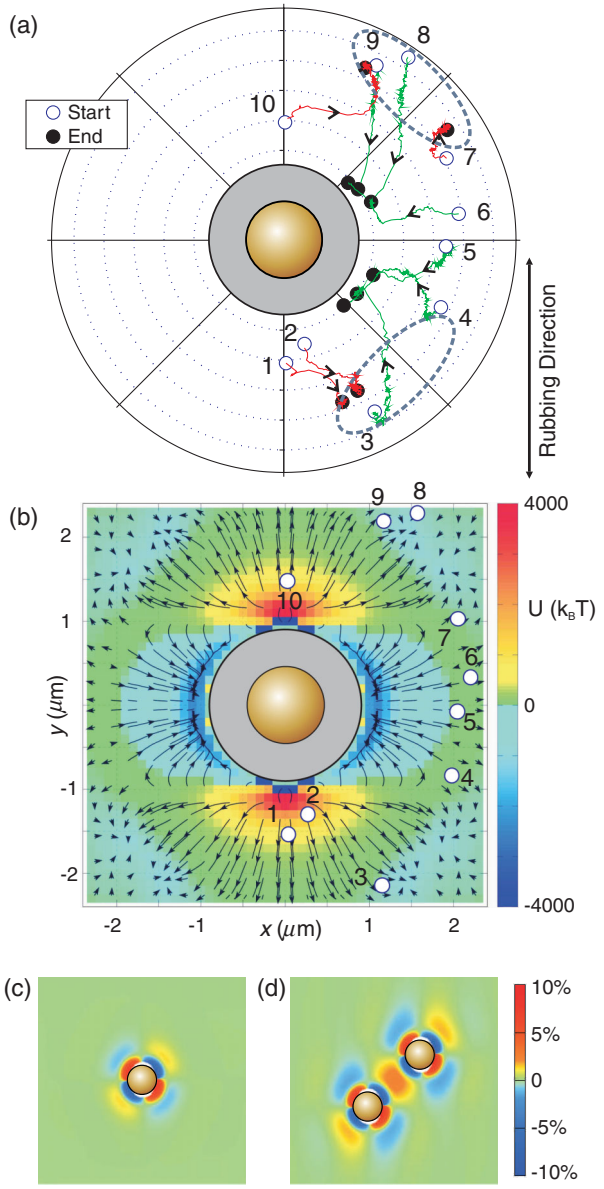

FIG. 4 (color online). Colloidal pair interaction in π-chiral nematic cell. One colloid is fixed in the origin, the other colloid, indicated by a circle, is approaching. (a) The set of 10 experiments with a pair of 4.7 μm silica particles in doped 5CB, with different starting positions. Note the starting and ending positions of colloids in different experiments. (b) The corresponding energy pair potential landscape, calculated within LdG model. The arrows indicate lines of force. (c), (d) The deviation of the $\pi/2$-twist helix length from the ideal half-cell-thickness. (c) A single particle and (d), a pair of particles. Red and blue colors denote compression of the top and the bottom half of the helix, respectively. The scale denotes the deviation of the vertical position where the director twists by $\pi/2$ relative to the bottom of the cell, in percents of the cell thickness.

chirality for colloidal interaction. While this work was focused on the colloidal interactions in two dimensions, we anticipate that chirality might play an important role for colloidal interactions in three dimensions. It was demonstrated recently that topological constraints and pair interaction are crucial for the assembly and control of 2D colloidal crystals [24] and we expect much richer physics in 3D chiral nematic colloidal crystals.

The authors thank Miha Ravnik for fruitful discussions. This work was supported by the European Commission Marie Curie project HIERARCHY Grant No PITN-GA-2008-215851 (V. S. R. J.), the Slovenian Research Agency (ARRS) Contract No. P1-0099 and No. J1-3612, and the Center of excellence NAMASTE.

[1] H. Stark, Phys. Rep. **351**, 387 (2001).
[2] P. Poulin, H. Stark, T. C. Lubensky, and D. A. Weitz, Science **275**, 1770 (1997).
[3] U. Tkalec, M. Ravnik, S. Žumer, and I. Muševič, Phys. Rev. Lett. **103**, 127801 (2009).
[4] B. Van Waeyenberge *et al.*, Nature (London) **444**, 461 (2006).
[5] I. Smalyukh, Y. Lansac, N. A. Clark, and R. P. Trivedi, Nat. Mater. **9**, 139 (2010).
[6] U. Tkalec, M. Ravnik, S. Čopar, S. Žumer, and I. Muševič, Science **333**, 62 (2011).
[7] V. S. R. Jampani, M. Škarabot, M. Ravnik, S. Čopar, S. Žumer, and I. Muševič, Phys. Rev. E **84**, 031703 (2011).
[8] J. S. Lintuvuori, K. Stratford, M. E. Cates, and D. Marenduzo, Phys. Rev. Lett. **105**, 178302 (2010).
[9] J. S. Lintuvuori, D. Marenduzo, K. Stratford, and M. E. Cates, J. Mater. Chem. **20**, 10 547 (2010).
[10] J. S. Lintuvuori, K. Stratford, M. E. Cates, and D. Marenduzo, Phys. Rev. Lett. **107**, 267802 (2011).
[11] R. P. Trivedi, I. I. Klevets, B. Senyuk, T. Lee, and I. I. Smalyukh, Proc. Natl. Acad. Sci. U.S.A. **109**, 4744 (2012).
[12] M. Zapotocky, L. Ramos, P. Poulin, T. C. Lubensky, and D. A. Weitz, Science **283**, 209 (1999).
[13] T. A. Wood, J. S. Lintuvuori, A. B. Schofield, D. Marenduzzo, and W. C. K. Poon, Science **334**, 79 (2011).
[14] N. Hijnen, T. A. Wood, D. Wilson, and P. S. Clegg, Langmuir **26**, 13 502 (2010).
[15] M. Škarabot, M. Ravnik, S. Žumer, U. Tkalec, I. Poberaj, D. Babič, N. Osterman, and I. Muševič, Phys. Rev. E **76**, 051406 (2007).
[16] J. C. Crocker and D. G. Grier, J. Colloid Interface Sci. **179**, 298 (1996).
[17] P. Poulin, V. Cabuil, and D. A. Weitz, Phys. Rev. Lett. **79**, 4862 (1997).
[18] M. Yada, J. Yamamoto, and H. Yokoyama, Phys. Rev. Lett. **92**, 185501 (2004).
[19] I. I. Smalyukh, O. D. Lavrentovich, A. N. Kuzmin, A. V. Kachynski, and P. N. Prasad, Phys. Rev. Lett. **95**, 157801 (2005).
[20] J. C. Loudet, A. M. Alsayed, J. Zhang, and A. G. Yodh, Phys. Rev. Lett. **94**, 018301 (2005).
[21] N. Osterman, Comput. Phys. Commun. **181**, 1911 (2010).
[22] M. Ravnik, G. P. Alexander, J. M. Yeomans, and S. Žumer, Faraday Discuss. **144**, 159 (2010).
[23] J.-i. Fukuda, B. I. Lev, and H. Yokoyama, Phys. Rev. E **65**, 031710 (2002).
[24] A. Nych, U. Ognysta, M. Škarabot, M. Ravnik, S. Žumer, and I. Muševič, Nat. Commun. **4**, 1489 (2013).